Journal of Power Sources 243 (2013) 72 77

Contents lists available at SciVerse ScienceDirect

Journal of Power Sources

journal homepage: www.elsevier.com/locate/jpowsour

Short communication

Dynamic *in situ* fourier transform infrared measurements of chemical bonds of electrolyte solvents during the initial charging process in a Li ion battery

Kenichi Hongyou, Takashi Hattori, Youko Nagai, Toshihiro Tanaka, Hiroyuki Nii, Kaoru Shoda*

UBE Scientific Analysis Laboratory, Inc., 1978-5, Kogushi, Ube-shi, Yamaguchi 755-8633, Japan

HIGHLIGHTS

- Solvation/desolvation and SEI formation at a graphite electrode during the initial charging process were investigated.
- We developed dynamic *in situ* FTIR measurement by applying a diamond ATR crystal.
- The measurement elucidated the change in the chemical bond of the electrolyte solvents in Li/electrolyte/graphite/Cu cell.
- The measurement also revealed the contribution of a vinylene carbonate additive to the electrolyte solvent reduction.

ARTICLE INFO

Article history:
Received 10 April 2013
Received in revised form
29 May 2013
Accepted 31 May 2013
Available online 10 June 2013

Keywords:
Li ion battery
Initial charging process
In situ FTIR
Solvation/desolvation
SEI formation
Li alkyl carbonate

ABSTRACT

Solvation/desolvation and the solid electrolyte interphase (SEI) formation at a graphite electrode during the initial charging process were investigated using *in situ* Fourier transform infrared spectroscopy (FTIR) measurements. These measurements were developed by applying a diamond attenuated total reflectance (ATR) crystal, which probed the electrolyte solvents at the surface of the graphite electrode and provided successive FTIR spectra with high signal to noise ratio. The charging process was performed in the Li(reference)/electrolyte/graphite(working)/Cu cell at a voltage ranging from 3.2 to 0.0001 V vs. Li/Li^+. The measurement elucidated the change in the chemical bond of the electrolyte solvents. In an early stage, the amounts of solvated and desolvated solvents changed, providing evidence that the Li^+ ions were intercalated into the graphite layer. The formation of the Li alkyl carbonate that forms the SEI layer was facilitated toward the end of the charging process. Measurements were also obtained of the elec trolyte with a vinylene carbonate additive, and the contribution of the additive to the electrolyte solvent reduction was investigated.

1. Introduction

The solid electrolyte interphase (SEI) on a graphite electrode plays important roles in the function of Li ion batteries; it prevents electrons from meeting Li^+ ions at the graphite surface during the charging process, and also prevents electro deposition which would severely deteriorate the battery performance [1]. In partic ular, the SEI formed during at the initial charging and discharging processes is known to be responsible for the battery's performance [2,3]. It has been reported that the SEI consists of organic and inorganic compounds; organic compounds such as Li alkyl carbonate were deposited on inorganic compounds such as LiF that were deposited on the surface of the graphite through the decomposition of electrolyte salts (for instance, $LiBF_4$ and $LiPF_6$) [4–6].

The organic compounds of the SEI were formed through the reduction and decomposition of electrolyte solvents [7–9]. During the charging process, Li^+ ions (emitted from cathode active mate rials) were solvated, diffused toward the graphite electrode by the electric field, desolvated at the surface of the graphite, and finally intercalated into the graphite layers [7,10]. The structure of the solvated solvents has also been investigated. For example, a theo retical calculation revealed that one Li^+ ion was coordinated to ethylene carbonate (EC) and dimethyl carbonate (DMC) molecules [11]. In order to understand the formation of the organic SEI, it is

* Corresponding author. Tel.: +81 836 31 6568; fax: +81 836 31 6601.
E-mail address: kaoru.shoda@ube-ind.co.jp (K. Shoda).

0378-7753/$ see front matter © 2013 Elsevier B.V. All rights reserved.
http://dx.doi.org/10.1016/j.jpowsour.2013.05.192

necessary to investigate the change in the chemical bonds of the electrolyte solvents at the surface of the graphite electrode during the initial charging process. Numerous approaches have been widely performed; however, it has been found that X ray photoelectron spectroscopy (XPS), widely used for the SEI analysis, provides little information on organic SEI and no information on the solvents [5,6]. Moreover, as the technique is performed under a vacuum, it only provides *ex situ* information. Although nuclear magnetic resonance (NMR) provides organic information on the solvents and can be performed during charging, it is unable to probe the solvents at the surface of the graphite electrode, only providing total information on the solvents [9,12].

Many effort investigations of the interface between the electrode and electrolyte solvents employing *in situ* Fourier transform infrared (FTIR) spectroscopy have been performed in order to understand the change in the electrolyte solvents [11,13–17]. However, they were conducted on metal electrodes such as Au, Pt, and Li due to various difficulties. To our knowledge, few *in situ* FTIR measurements have been obtained at the surface of graphite electrodes during the charging and discharging processes. For instance, infrared reflection absorption spectroscopy (IRAS) provides a tiny intensity of reflected light, demanding an increased signal to noise (S/N) ratio to analyze the signals by means of subtractively normalized interfacial FTIR Spectroscopy (SNIFTIRS) [13,17]. Since SNIFTIRS provides the difference spectrum between the sample and reference spectra, it neglects the peak shift. The attenuated total reflectance (ATR) FTIR technique has also been applied to *in situ* FTIR measurements; this method commonly uses a Ge crystal because its high refractivity gives a high S/N ratio spectra [13,17]. However, Ge reacts with Li to form an alloy around 0 V vs. Li/Li^+ during the charging process, leading to failure of the *in situ* FTIR measurements.

In this study, we applied a diamond ATR crystal to the *in situ* FTIR measurement. Diamond is electrochemically inactive during the charging process. We investigated the chemical bond change in the electrolyte solvents at the surface of the graphite in the Li(reference)/electrolyte/graphite(working)/Cu cell. In the initial charging process, the voltage ranged from 3.2 to 0.0001 V vs. Li/Li^+. At a voltage between 3.2 and 0.5 V, we observed the desolvation of the solvated Li^+ ions at the surface of the graphite from the high S/N ratio FTIR spectra, which supported the previous reports [7,8,10]. At a voltage between 0.5 and 0.05 V, the solvated and desolvated solvents were nearly constant in amount, which meant that the desolvation balanced the diffusion of the solvated Li^+ ions. At a voltage between 0.05 and 0.0001 V, we clearly observed the transform of the solvents into the Li alkyl carbonate, suggesting that the organic SEI formation was promoted at the late stages of the initial charging process. We also applied the *in situ* FTIR measurement to the electrolyte with a vinylene carbonate (VC) additive, and clearly showed that the additive prevented the formation of the Li alkyl carbonate at the surface of the graphite electrode.

2. Experimental

2.1. Battery cell fabrication

A graphite electrode was fabricated by a coating slurry of 90% (w/w) graphite and 10% (w/w) PVdF binder in *N* methylpyrolidone on both sides of a copper foil. The copper foil contained paths of the electrolyte, which allowed us to acquire *in situ* FTIR spectra during the charging and discharging processes. After drying, a graphite electrode disk with a diameter of 14 mm was used as a working electrode. Li foil was employed as both reference and counter electrodes. The graphite and Li electrodes were separated by glass wool and the electrolyte. The electrolyte was composed of battery grade dimethyl carbonate (DMC), diethyl carbonate (DEC), and ethylene carbonate (EC) (1:1:1 in v/v) with 1.0 M $LiPF_6$ (UBE industries Ltd.) without further purification. The water contents of DMC, DEC, and EC were less than 20 ppm.

2.2. In situ FTIR measurement

The *in situ* FTIR measurements were performed using an Agilent FTS 7000e FTIR spectrometer equipped with a liquid nitrogen cooled mercury cadmium telluride detector. The spectrometer was equipped with a single reflectance mode of the ATR sampling apparatus (Specac Ltd.) used for the charging and discharging processes, as shown in Fig. 1. The sampling apparatus was covered with a plastic cylinder, which enables the measurement to be performed under inactive conditions without an atmospheric effect. The battery cell was placed on the diamond prism, and then the electrolyte was added into the apparatus in an argon globe box having a dew point lower than −60 °C. After the apparatus was removed from the globe box, it was set into the FTIR spectrometer. The angle of incident light was set to 45°. The measurements were conducted in a kinetics mode at room temperature, and one spectrum was acquired every second. Since the average of the spectra was obtained from a 60 s measurement at each point, the signal intensity was enough large to be analyzed without the spectrum correction. The spectra were recorded at a resolution of 4 cm^{-1} between 650 and 4000 cm^{-1}, and they were analyzed in detail between 1600 and 1900 cm^{-1}.

It was noticed that a theoretical penetration depth of the incident light ranges from 1.1 μm (1900 cm^{-1}) to 1.3 μm (1600 cm^{-1}). This means that it is necessary to decrease the distance between the diamond crystal and the graphite electrode for probing information in the vicinity of the graphite electrode. Therefore, the cell was pushed against the diamond crystal and the graphite electrode was placed very close to the diamond crystal. Though we were concerned that the electrolyte might be restricted in its diffusion to the graphite electrode because of the narrow space, the electrolyte solution was able to diffuse through the intrinsic surface roughness of the graphite electrode, thereby continuing the electrochemical reaction.

2.3. Estimation of solvation and desolvation from FTIR spectra

In order to distinguish between the solvation and desolvation of the solvents from the FTIR spectra, single mode ATR measurements were conducted on DMC, DEC, and EC, both with and without 1.0 M $LiPF_6$. Typical spectra obtained from the *in situ* FTIR measurements

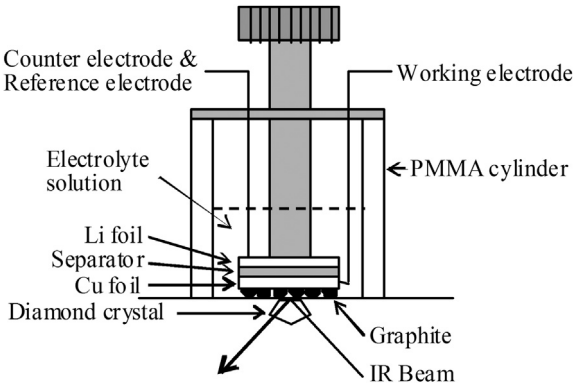

Fig. 1. Schematic illustration of the *in situ* FTIR apparatus. The battery cell was fabricated in the sampling ATR apparatus, where a graphite electrode formed on both sides of the Cu foil that contained paths of the electrolyte.

were analyzed by the deconvolution method which is widely used in XPS analysis [18].

2.4. Electrochemical measurement

Potential control and current measurement were performed with an ALS 760D potentiostat, connected to a personal computer. After ensuring that the cell had an open circuit potential (OCP) of up to 3.2 V vs. Li/Li$^+$, a user created electrochemical measurement program was used to obtain the electrochemical measurements at room temperature. The electrochemical condition is detailed in Fig. 4(a) in the next section.

3. Results and discussion

3.1. Solvation and desolvation of electrolyte solvents

Single reflection ATR FTIR measurements were conducted for the individual electrolyte solution in order to assign peaks due to DMC, DEC, and EC. Fig. 2(a)–(c) shows the FTIR spectra of DMC, DEC, and EC, respectively, both with (dashed lines) and without (solid lines) $LiPF_6$. Since no peaks from $LiPF_6$ were detected in wave numbers from 1100 to 1900 cm^{-1}, all peaks were assigned to the solvated and desolvated solvents.

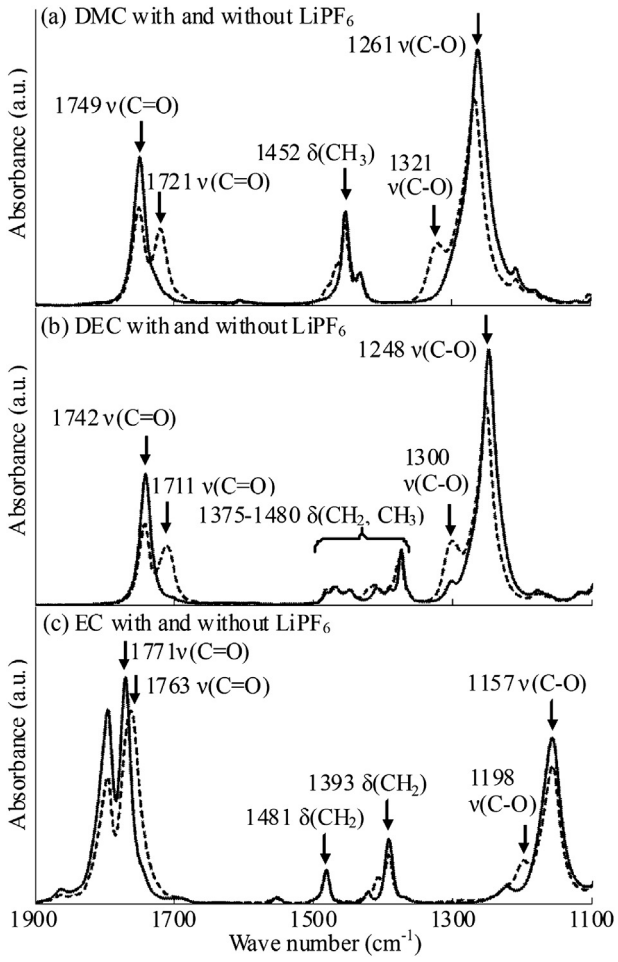

Fig. 2. FTIR spectra of (a) DMC, (b) DEC, and (c) EC, both with (dashed lines) and without (solid lines) $LiPF_6$. The peaks at 1742, 1749, and 1771 cm ^{1} in DEC, DMC, and EC (that were attributed to the C=O stretching vibration) shifted to 1711, 1721, and 1763 cm ^{1}, respectively. These shifts show the solvation in the presence of $LiPF_6$.

It was clear that the addition of $LiPF_6$ changed the FTIR spectra. In DMC, shown in Fig. 2(a), the peaks at 1721 and 1749 cm^{-1} were observed in the presence of $LiPF_6$, and they were attributed to the C=O stretching vibration mode [11]. The peak at 1721 cm^{-1} was not detectable in the absence of $LiPF_6$ and appeared in the presence of $LiPF_6$. This provided evidence that the C=O of the DMC molecules was weakly bound to the Li^+ ions dissociated from $LiPF_6$ by an electrostatic force, and consequently the C=O vibration mode shifted to the lower frequency side. These phenomena were also observed in previous works [11,17], and they were attributed to the molecular solvation to Li^+ ions. Therefore, FTIR spectroscopy distinguished between the solvated and desolvated DMC. The peaks around 1452 cm^{-1} were attributed to the C–H_3 bending vibration mode, and they barely differed from each other. The peaks at 1261 and 1321 cm^{-1} were attributed to the C–O stretching vibration mode; the latter was only observed in the presence of $LiPF_6$. The shift of the C–O bonding peak to a higher frequency in the presence of $LiPF_6$ was also observed in a previous report [11]. Similar peak shifts were observed in DEC as shown in Fig. 2(b). In EC, shown in Fig. 2(c), similar peak shifts were observed between 1100 and 1500 cm^{-1}, and the peak of the C=O stretching vibration mode at 1771 cm^{-1} slightly shifted to 1763 cm^{-1}, making it difficult to distinguish the solvated EC from the desolvated EC with the FTIR spectra as there was only a small difference in wave number.

As discussed above, the peaks between 1742 and 1749 cm^{-1} corresponded to the C=O vibration mode of DEC and DMC, and the peaks between 1711 and 1721 cm^{-1} corresponded to the mode weakly bound to Li^+ ions. Therefore, we focused on the FTIR spectra between 1600 and 1900 cm^{-1}. Fig. 3 (a) and (b) shows typical FTIR spectra obtained from the *in situ* FTIR measurements before the charge and after 90% of the charge, respectively. The spectra consisted of the solvated and desolvated DMC, DEC, and EC. In order to clearly discern the solvation and desolvation, the spectra were deconvoluted to seven peaks on the basis of the spectra in Fig. 2, as indicated by the dashed lines in Fig. 3. Table 1 shows the ratios of the deconvoluted peak intensity to the total intensity. The peaks at 1775 and 1806 cm^{-1} were attributed to the solvated and desolvated EC. The broad peak at 1746 cm^{-1} was attributed to the desolvated DMC and DEC, and the shoulder peak at 1717 cm^{-1} was attributed to the solvated DMC and DEC. It was expected that the spectra in the presence of DEC, DMC, and EC did not coincide with those in the presence of one solvent, because more than two solvent molecules interacted with one Li^+ ion [7,10,11], and could cause small changes in wave number and shape. Therefore, we did not quantitatively discuss the solvation and desolvation of the solvents, but qualitatively estimated them to determine the change in chemical bond of the solvents.

The broad peak at 1657 cm^{-1} was barely recognizable in Fig. 3(b). This peak was attributed to the C=O stretching vibration mode of the Li alkyl carbonate, such as $(CH_2OCO_2Li)_2$ [19] and $ROCO_2Li$ [20], which was formed by the reduction of electrolyte solvents during electrochemical reactions.

3.2. Charging process

Fig. 4(a) shows the voltammetric curves of the *in situ* FTIR measurement during the initial charging process. The charging process was controlled at a constant current of 0.33 mA cm^{-2} from 3.2 to 0.0001 V vs. Li/Li$^+$, and then converted to a constant voltage condition for 120 min.

The charging process was classified into five regions, denoted as I, II, III, IV, and V in Fig. 4(a). The voltage linearly decreased from 3.2 to 0.5 V in region I, and then plateaued at 0.5 V in region II. In regions III and IV, the voltage monotonically decreased from 0.5 to 0.05 V followed by a small decrease from 0.05 to 0.0001 V, respectively. In region V, the current gradually decreased at a

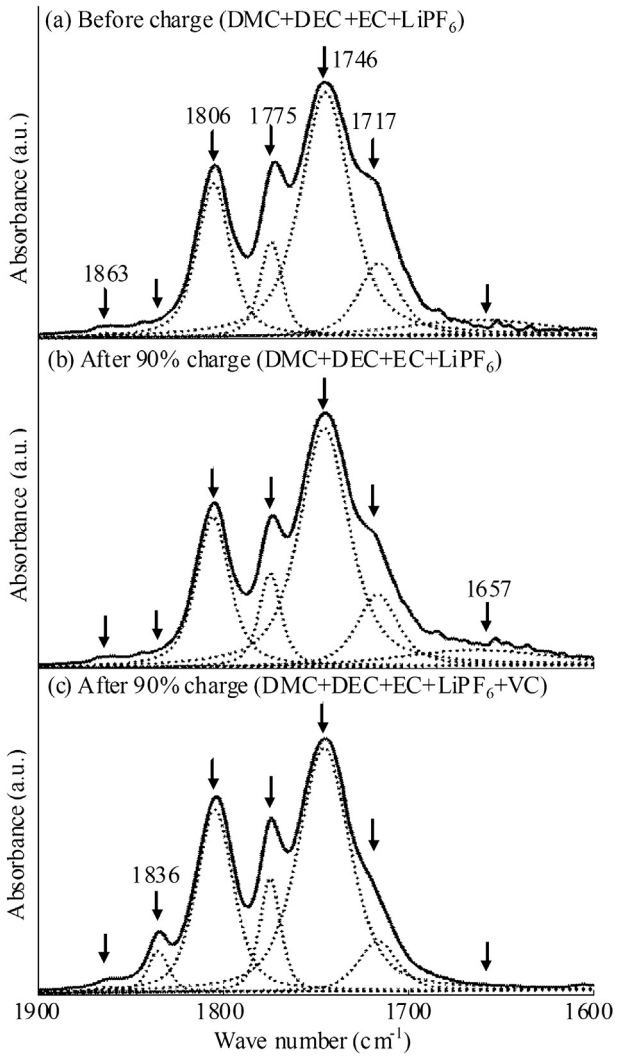

Fig. 3. FTIR spectra (a) before charge, (b) after 90% charge without VC additive, and (c) after 90% charge with VC additive. The spectra were deconvoluted and separated into seven peaks based on the spectra shown in Fig. 2, and the peak intensity ratios were summarized in Table 1. The peaks at 1657, 1717, and 1746 cm ^{1} were attributed to the Li alkyl carbonate, solvated DMC and DEC, and desolvated ones, respectively. The peak at 1836 cm ^{1} was attributed to the C=O vibration mode of VC.

constant voltage of 0.0001 V. The curve in Fig. 4(a) shows similar characteristics to those obtained from a Li ion battery. This meant that the electrochemical reaction ran efficiently throughout the charging process.

3.3. Change in the chemical bond of electrolyte solvents during the initial charging process

In order to determine electrochemical reaction within the initial charging process, we obtained FTIR spectra every minute (Fig. 3(a) and (b)). The peak intensities corresponding to the absorbance at 1657, 1717, and 1746 cm^{-1} were plotted as a function of the charging time, as shown in Fig. 4(b); they corresponded to the C=O bond in Li alkyl carbonate, that in the solvated DMC and DEC, and that in the desolvated DMC and DEC. In Fig. 4(b), the magnitude of the vertical axis changed to allow an easy comparison of the change in individual peak intensity. The peak intensities showed successive changes during the charging process, which revealed the changes in the bond of the electrolyte solvents, namely the solvation, desolvation, and reduction. Therefore, here we discuss what occurred at the surface of the graphite electrode.

It was noticed that the electrostatic field at both sides of the graphite electrode were different from each other, as shown in Fig. 1, and this influenced the ionic diffusion coefficient. The diffusion velocity of the solvated solvents at the outer electrode was probably smaller than that at the inner electrode. Consequently, the ratio of the solvated and desolvated solvents at the outer electrode was assumed to be different to some extent from the ratio at the inner electrode. Indeed, the capacity of the cell was <200 mA hg^{-1}, which was smaller than the usable capacity of graphite as an anode, about 300 mA hg^{-1}. However, it was assumed that the difference in the diffusion had little influence on the primitive electrochemical reaction mechanism.

In region I, where the voltage rapidly decreased from 3.2 to 0.5 V, the peak intensity at 1717 cm^{-1} linearly decreased and that at 1746 cm^{-1} linearly increased; thus, the solvated solvents decreased and the desolvated solvents increased. It was clear that the solvated Li^{+} ions diffused to the graphite electrode and they were intercalated into graphite layers with accompanying desolvation, as previously reported [7]. If the solvated Li^{+} ions were intercalated without desolvation, which would cause to exfoliation of the graphite layers [3], the desolvated solvents would not increase. Therefore, it was assumed that exfoliation rarely occurred in this region. After the solvated Li^{+} ions were desolvated at the surface of the graphite electrode, additional solvated Li^{+} ions and those desolvated solvents diffused to and from the electrode, respectively, by the concentration gradient that was probably produced at the vicinity of the electrode. In order to precisely understand the change in the solvated and desolvated solvents, it was necessary to consider the diffusion of the solvents, as discussed below. It was confirmed that electrolyte solvents were desolvated at the surface of the electrode in the early stage of the charging process.

In region II, with a plateau at a voltage of about 0.5 V, the peak intensity at 1717 cm^{-1} continued to decrease and that at 1746 cm^{-1} increased. It has been reported that the organic SEI formation was initiated through the reduction of solvents such as EC to create Li alkyl carbonate at this voltage [2,16]. However, the peak intensity around 1657 cm^{-1} rarely increased. It was thought that the amount of Li alkyl carbonate was too small to be efficiently detected. Tasaki et al. [8] found that the solubility of $LiOCO_2C_2H_5$ and $LiOCO_2CH_3$ in DMC was 50–70 ppm. This meant that parts of the formed Li alkyl carbonate could dissolve in the electrolyte and deposit on the graphite electrode forming the organic SEI. It was assumed that the desolvation continued at the surface of the graphite electrode and the formation of the organic SEI probably began to occur in this region.

Table 1
The ratios of the peak intensities (at 1657, 1717, 1746, 1775, and 1806 cm ^{1} obtained from the FTIR spectra in Fig. 3 by the deconvolution method) to the total intensities of the seven peaks. A ratio of 0.11% at 1657 cm ^{1} before charge was background noise level. VC additive clearly prevented the electrolyte solvents from being reduced into the Li alkyl carbonate at the surface of the graphite electrode.

FTIR spectrum	1657 cm ^{1}	1717 cm ^{1}	1746 cm ^{1}	1775 cm ^{1}	1806 cm ^{1}
Before charge (DMC + DEC + EC + $LiPF_6$)	0.11%	17.16%	49.91%	10.79%	21.59%
After 90% charge (DMC + DEC + EC + $LiPF_6$)	9.75%	12.04%	48.67%	8.51%	20.51%
After 90% charge (DMC + DEC + EC + $LiPF_6$ + VC)	0.00%	7.98%	51.25%	9.59%	27.08%

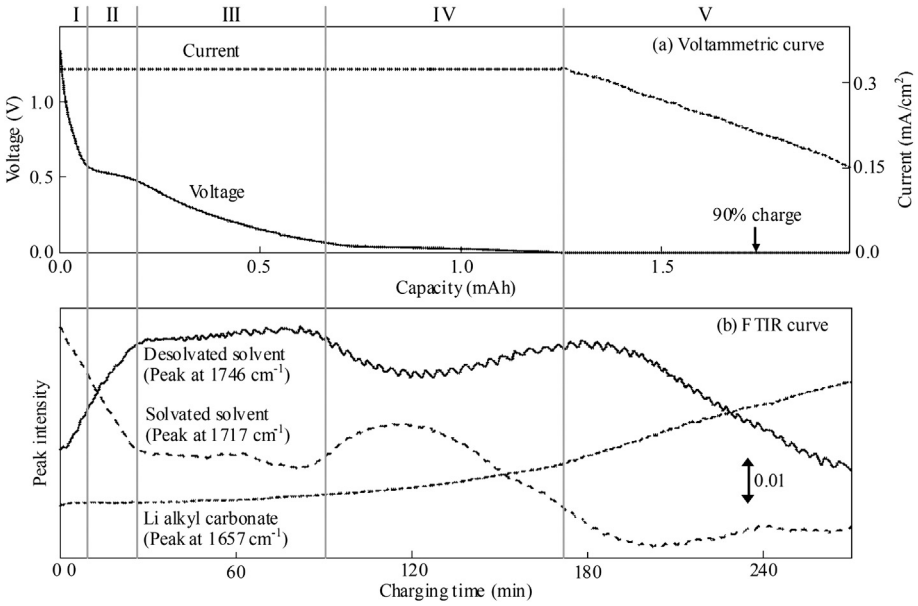

Fig. 4. (a) Voltammetric curve showing the voltage and current as a function of the charging capacity, and (b) FTIR curve showing the peak intensities at 1657, 1717, and 1746 cm ^{1} as a function of the charging time, where the peak intensity corresponded to the absorbance of the peaks. In (b), the magnitudes of the vertical axis of the three peaks were different from each other and the rate of change of the vertical axis was constant. The charging process was classified into five regions according to the voltammetric curve. FTIR spectra before charge and after 90% charge, designated by the arrow in (a), are shown in Fig. 3(a) and (b), respectively.

In region III, where the voltage monotonically decreased from 0.5 to 0.05 V, the peak intensities at 1717 and 1746 cm^{-1} were nearly constant, showing that the desolvated solvents were balanced with the solvated ones supplied through the diffusion. In addition, the peak intensity at 1657 cm^{-1} started to increase gradually, which provided evidence that the desolvated solvents gradually participated in the formation of the organic SEI layer. Since the layer tended to resist Li^+ ions passing through it, the desolvation was supposed to be suppressed at the surface of the SEI layer. It was suggested, therefore, that the diffused solvated sol vents were gradually desolvated at the surface of the graphite electrode with the formation of the organic SEI layer, showing that the amounts of the solvated and desolvated solvents appeared to be constant.

In region IV, where the voltage gradually decreased from 0.05 to 0.0001 V, the sum of the peak intensities of the solvated and des olvated solvents was not constant but gradually decreased; this was explained by the rapid increases in the peak intensity at 1657 cm^{-1}. This meant that the formation of the SEI layer accelerated as the resistance of the Li^+ ions increased. Since the current was constant, electrons were assumed to be used as the reduction of the solvents that formed a thick SEI layer as well as the intercalation of Li^+ ions into graphite layers. Therefore, it was supposed that the variation of the peak intensities at 1717 and 1746 cm^{-1} was influenced by not only the supply of the solvated solvents to the surface of the graphite electrode, but also by the consumption of the formation of the SEI layer.

In region V, with a constant voltage of 0.0001 V, the desolvated solvents gradually decreased after a slight increase. In addition, the solvated solvents gradually decreased and remained at a low level, and the Li alkyl carbonate rapidly increased. The decrease in the signal intensity of the solvents possibly resulted from the decrease in the volume of electrolyte at the space between the graphite electrode and diamond window; the volume fraction of SEI layer was increased by the irreversible decomposition of solvents, and the volume expansion of graphite electrode took place. Although these volume changes may have weakened the signal intensity, the rapid increase in the intensity of the Li alkyl carbonate provided evidence that the SEI layer prevented the Li^+ ions from being effi ciently intercalated into graphite layer, causing the current to decrease gradually at the setting voltage. Toward the end of the charging process, the consumption of the desolvated solvents was dominated by the formation of the Li alkyl carbonate. It was concluded that the reduction of the desolvated solvents produced a thick organic SEI layer, deteriorating the characteristics of the SEI layer.

As shown above, the *in situ* FTIR clearly demonstrated the solvation and desolvation of the electrolyte solvents, as well as the formation of the Li alkyl carbonate that formed the organic SEI at the surface of the graphite electrode during the initial charging process. These results explain the voltammetric curves. In the early stage, the amount of the solvated and desolvated solvents changed, which was likely due to the intercalation of Li^+ ions into the graphite layer. The solvated and desolvated solvents were balanced at the next stage, and the formation of the SEI layer was facilitated toward the end of the charging process. Hence, this system was able to elucidate the phenomena of the change in chemical bond of the electrolyte solvents, and especially may contribute to improved charging conditions for the SEI formation since it directly monitored the reduction of the electrolyte solvents.

3.4. Effect of VC additive on changes in the chemical bond of electrolyte solvents

It has been reported that the performance of Li ion batteries is improved via the addition of additives such as olefinic compounds [2], vinylene carbonate (VC) [16,21], and fluoroethylene carbonate [22] to the electrolyte. Of these additives, VC decreased the reductive gas and increased the thermal decomposition tempera ture of the electrolyte. These improvements were closely related to the characteristics of the SEI layer. Hence, we investigated the effect of the addition of a VC additive to the electrolyte on changes in the chemical bond of the electrolyte solvents.

A VC was added to the electrolyte as mentioned above at 5% (w/w). The *in situ* FTIR measurement was performed under an

electrochemical condition similar to Fig. 4(a). Fig. 3(c) shows the FTIR spectrum after 90% of the charge, where the peak at 1836 cm^{-1} was attributed to the C═O stretching vibration of VC. Table 1 shows the ratios of the deconvoluted peak intensities to the total intensities. The formation of the Li alkyl carbonate that appeared at 1657 cm^{-1} was clearly suppressed. Therefore, the VC additive contributed to a decrease in the reduction or decomposition of the electrolyte solvents, which improved the characteristics of the SEI layer and the capacity of the cell.

4. Conclusions

In order to understand the solvation, desolvation, and SEI formation of electrolyte solvents, we developed an *in situ* FTIR measurement by applying a diamond ATR crystal to the FTIR apparatus. We were then able to probe the electrolyte solvents at the surface of the graphite electrode during the charging process from 3.2 to 0.0001 V vs. Li/Li^+. The measurement provided successive FTIR spectra with high S/N ratio, and consequently the spectra were directly analyzed without correction. Based on the FTIR spectra of individual solvents, both with and without $LiPF_6$, it was recognized that the solvation and desolvation of the electrolyte solvents with Li^+ ions could be analyzed.

The *in situ* FTIR measurement elucidated the change in the chemical bond of the electrolyte solvents, as follows. In the early stage of the charging process, the solvated and desolvated solvents changed in quantity, which provided evidence that the desolvation occurs at the surface of the graphite electrode. As the charging process proceeded, the solvated and desolvated solvents became balanced. The formation of the Li alkyl carbonate that formed the SEI layer was facilitated toward the end of the charging process. In addition, we applied the measurement to the electrolyte with a VC additive and showed that the formation of the Li alkyl carbonate was suppressed, leading to an improvement of the SEI layer. Therefore, the measurement technique was widely applicable to the investigation of the phenomena in Li ion batteries, and especially contributed an improvement in the charging condition of the SEI formation.

References

[1] E. Peled, J. Electrochem. Soc. 126 (1979) 2047.
[2] K. Abe, H. Yoshitake, T. Kitakura, T. Hattori, H. Wang, M. Yoshino, Electrochim. Acta 49 (2004) 4613.
[3] W. Markle, C.-Y. Lu, P. Novak, J. Electrochem. Soc. 158 (2011) A1478.
[4] A.M. Andersson, K. Edstrom, J. Electrochem. Soc. 148 (2001) A1100.
[5] K. Edstrom, M. Herstedt, D.P. Abraham, J. Power Sources 153 (2006) 380.
[6] R. Dedryvere, H. Martinez, S. Leroy, D. Lemordant, F. Bonhomme, P. Biensan, D. Gonbeau, J. Power Sources 174 (2007) 462.
[7] X. Kang, L. Yiufai, S.Z. Sheng, J.T. Richard, B.C. Timothy, J. Phys. Chem. C 111 (2007) 7411.
[8] K. Tasaki, A. Goldberg, J.-J. Lian, M. Walker, A. Timmons, S.J. Harris, J. Electrochem. Soc. 156 (2009) A1019.
[9] G. Gachot, S. Grugeon, M. Armand, S. Pilard, P. Guenot, J.-M. Tarascon, S. Larulle, J. Power Sources 178 (2008) 409.
[10] K. Leung, J.L. Budzien, Phys. Chem. Chem. Phys. 12 (2010) 6583.
[11] Y. Ikezawa, H. Nishi, Electrochim. Acta 53 (2008) 3663.
[12] N.M. Trease, L. Zhou, H.J. Chang, B.Y. Zhu, C.P. Grey, Solid State Nucl. Magn. Reson. 42 (2012) 62.
[13] E. Goren, O. Chusid, D. Aurbach, J. Electrochem. Soc. 138 (1991) L6.
[14] D. Aurbach, B. Markovsky, M.D. Levi, E. Levi, A. Schechter, M. Moshkovich, Y. Cohen, J. Power Sources 81–82 (1999) 95.
[15] M. Moshkovich, M. Cojocaru, H.E. Gottlieb, D. Aurbach, J. Electrochem. Soc. 497 (2001) 84.
[16] H. Ota, Y. Sakata, A. Inoue, S. Yamaguchi, J. Electrochem. Soc. 151 (2004) A1659.
[17] T. Matsushita, K. Dokko, K. Kanamura, J. Power Sources 146 (2005) 360.
[18] S. Kundu, Y. Wang, W. Xia, M. Muhler, J. Phys. Chem. C 112 (2008) 16869.
[19] L.J. Rendek, G.S. Chottiner, D.A. Scherson, Langmuir 17 (2001) 849.
[20] T. Abe, H. Fukuda, Y. Iriyama, Z. Ogumi, J. Electrochem. Soc. 151 (2004) A1120.
[21] M. Herstedt, H. Rensmo, H. Siegbahn, K. Edstrom, Electrochim. Acta 49 (2004) 2351.
[22] I.A. Profatilova, S.-S. Kim, N.-S. Choi, Electrochim. Acta 54 (2009) 4445.